A study of tidal and planetary wave periodicities present in midlatitude sporadic *E* layers

Christos Haldoupis
Physics Department, University of Crete, Iraklion, Crete, Greece

Dora Pancheva and N. J. Mitchell
Department of Electronic and Electrical Engineering, University of Bath, Bath, UK

Received 27 September 2003; revised 5 November 2003; accepted 13 November 2003; published 5 February 2004.

[1] The diurnal and semidiurnal atmospheric tides are known to be of fundamental importance in the formation of midlatitude sporadic *E* layers, acting through their vertical windshear forcing of the long-living metallic ions in the lower thermosphere. Also, recent studies suggested that planetary waves play a role on sporadic *E* generation as well, a fact that went unnoticed in the long-going research of sporadic layers. In this paper a methodology is employed to investigate the tidal and planetary wave periodicities imprinted onto sporadic *E* critical frequencies *foEs*. In this approach, standard analysis techniques used in neutral atmospheric dynamics are applied on *foEs* time series obtained during summertime when sporadic *E* occurrence is nearly continuous. It is shown that besides the dominant and known 24-hour and 12-hour tidal periodicities in *foEs*, there is often a weaker terdiurnal (8-hour) oscillation present as well. In addition, there are planetary wave periodicites in *foEs* with periods near the normal Rossby modes, that is, 2, 5, 10, and 16 days. It is also found that the tidal oscillations in *foEs* undergo a strong amplitude modulation with periods comparable to the dominant planetary wave periodicities present in the data. Our results are in line with recent findings based on a single event study which suggested that sporadic *E* layers are affected indirectly by planetary waves through their nonlinear interaction and modulation of the atmospheric tides at lower altitudes. The close relationship between neutral wave dynamics and midlatitude sporadic *E* periodicities suggests that the ionosonde data can be used as an alternative means of studying tidal and planetary wave characteristics and their climatology in the lower thermosphere. *INDEX TERMS:* 2439 Ionosphere: Ionospheric irregularities; 2427 Ionosphere: Ionosphere/atmosphere interactions (0335); 3384 Meteorology and Atmospheric Dynamics: Waves and tides; 2443 Ionosphere: Midlatitude ionosphere; *KEYWORDS:* ionosphere-atmosphere interactions, metallic ion layers, midlatitude ionosphere, waves and tides, nonlinear interactions

Citation: Haldoupis, C., D. Pancheva, and N. J. Mitchell (2004), A study of tidal and planetary wave periodicities present in midlatitude sporadic *E* layers, *J. Geophys. Res.*, *109*, A02302, doi:10.1029/2003JA010253.

1. Introduction

[2] The midlatitude sporadic *E*, or temperate E_s, are dense layers of metallic ions which form mostly in the lower thermosphere between 90 and 120 km, a region that is characterized by complicated atmospheric dynamics and nonlinear plasma processes. The sporadic *E* phenomenon, which is representative of the complex interaction between the neutral atmosphere and the ionosphere, has attracted considerable attention over the last decades, which led to numerous scientific studies. In our present understanding, the formation of E_s relies on vertical wind shears associated with atmospheric tides and gravity waves that force the long-living metallic ions into thin layers. For a summary of E_s properties and a large list of references, see reviews by *Whitehead* [1989] and *Mathews* [1998].

[3] Although temperate sporadic *E* have been studied primarily with ionosondes, in the last 2 decades new knowledge was obtained with the incoherent scatter radar (ISR) at Arecibo. As summarized by *Mathews* [1998], the Arecibo studies revealed a parenting process for the "classical" sporadic *E* in the lower *E* region which involves descending "intermediate" layers that initiate in the upper *E* and lower *F* regions. Furthermore, the Arecibo observations established a fundamental role for the diurnal and semidiurnal tides in E_s formation, which often are also referred to as "tidal ion layers." The contribution of 12-hour and 24-hour tides on E_s formation has been identified also in ionosonde records [e.g., see *MacDougall*, 1974; *Wilkinson*

0148-0227/04/2003JA010253$09.00

et al., 1992; *Szuszczewicz et al.*, 1995]. Moreover, both ISR and ionosonde studies suggested that E_s is part of a deterministic rather than a sporadic process, which involves regular wind shear convergence and downward transport in the context of the global system of thermospheric tides.

[4] Besides the tides, gravity waves with periods from a few hours down to the Brunt-Vaisala period of 5 min must also play a role in E_s generation. Obviously, there is a wealth of gravity waves in the lower thermosphere that have amplitudes and wind shears sufficiently large to affect the vertical motion of plasma locally or even increase/decrease horizontal transport within the layer itself [e.g., see *Chimonas*, 1971]. Gravity waves can intervene and alter the regular tidal forcing of the E_s forming process; therefore their confluence with tidal waves can reinforce or disrupt the convergence of metallic plasma into a layer and thus impose a sporadic character in E_s. Naturally, the unpredictable occurrence of gravity waves combined with their dynamic evolution and breaking at lower thermospheric heights makes it difficult for their effects on E_s to be quantified.

[5] In addition to the anticipated role of atmospheric tides and gravity waves, recent results suggested that planetary waves (PW) play a role on E_s formation as well [e.g., see *Tsunoda et al.*, 1998; *Voiculescu et al.*, 1999; *Igarashi and Kato*, 2001]. The first direct evidence for a link between E_s and PW was provided by *Haldoupis and Pancheva* [2002]. They used sporadic *E* layer critical frequency (*foEs*) data from an extended longitudinal chain of ionosondes during a strong PW event that occurred in August–September 1993 to show that all stations displayed the same 7-day periodicity in *foEs* concurrently with the 7-day PW found independently in MLT ground radar and satellite wind measurements [*Clark et al.*, 2002; *Wu et al.*, 1994; *Meyer and Forbes*, 1997]. In an effort to understand the E_s-PW relationship, *Pancheva et al.* [2003] correlated MLT wind and ionosonde *foEs* time series for the same 7-day PW event. They found that E_s was affected by the planetary waves indirectly through the action of the diurnal and semidiurnal tides, which were modulated by their nonlinear interaction with the PW at subsporadic *E* altitudes.

[6] The present study comes as a continuation of recent work on tidal and planetary wave effects on midlatitude sporadic *E* layers. Actually, it was triggered by the need to test the validity and generality of the findings based on the strong 7-day PW event of August–September 1993. Here, a methodology is developed and used to identify and quantify the tidal and PW periodicities impacted upon sporadic *E* and then investigate their temporal evolution and how the long-period amplitude modulation in the tidal periodicities compares with the PW oscillations present also concurrently in the data.

[7] In the following, we first set the stage by providing the basics of windshear theory as applies at midlatitude. Then the objective of this work is stated briefly followed by the description of the data and analysis methods. The results are then presented in the subsequent sections, and the main findings are summarized and discussed in the last part of the paper.

2. Basics of Windshear Theory

[8] Our understanding of sporadic *E* formation relies on the so-called "windshear theory" first introduced in the 1960s and developed further in the following years (for a list of references see review by *Whitehead* [1989]). This theory shows that vertical wind shears with a proper polarity can cause, by the combined action of ion-neutral collisional coupling and geomagnetic Lorentz forcing, the long-lived metallic ions to move vertically and converge into dense plasma layers. In this process, the magnetized electrons simply follow the ions by moving along the field lines to maintain charge neutrality.

[9] In general, the driving agents which act to form the layers are both winds and electric fields, but at midlatitude the ambient dynamo electric fields are small and have a minimal contribution relative to the winds; thus they are omitted. The theory relies on the steady state ion momentum equation which, after neglecting diffusion and electric field forces, takes the simplified form:

$$e\mathbf{v}_i \times \mathbf{B} + M\nu_i(\mathbf{v}_i \times \mathbf{U}) = 0, \tag{1}$$

where e and M are the ion charge and ion mass; ν_i is the ion-neutral collision frequency; and $\mathbf{v}_i$, $\mathbf{B}$, and $\mathbf{U}$ are the ion velocity, magnetic field, and neutral wind velocity vectors, respectively.

[10] Following the notations of *Mathews and Bekeny* [1979], one arrives easily from equation (1) to the vertical drift velocity of ions (positive upwards):

$$w_z = \frac{\cos I \sin I}{1 + (\nu_i/\omega_i)^2} U + \frac{(\nu_i/\omega_i)\ \cos I}{1 + (\nu_i/\omega_i)^2} V, \tag{2}$$

where U and V are the geomagnetic southward and eastward components of the neutral wind (representing approximately the meridional and zonal wind components, respectively), I is the magnetic dip angle, and $(\nu_i/\omega_i) = r$ is the ratio of ion-neutral collision frequency to ion gyrofrequency. The vertical winds are ignored as being too small to have a significant effect on vertical plasma transport.

[11] The vertical plasma drift becomes collision-dominated below about 125 km because $r^2 \gg 1$. The meridional wind (first) term in equation (2) dominates over the zonal wind (second) term above say 125 km, where r becomes increasingly smaller than unity as the ions become less and less collisional with increasing altitude. Thus in the upper *E* region the meridional winds play the dominant role in vertical plasma convergence with layers forming most effectively in the presence of a suitable meridional wind shear, that is, with a northward wind above and a southward or smaller northward wind below. On the other hand, below about 120 km the vertical plasma motion is controlled solely by the zonal wind, with a downward (upward) drift caused by a westward (eastward) wind. In this case the plasma convergence into a layer becomes effective in the presence of a vertical wind shear with a westward wind above and an eastward or smaller westward wind below.

[12] Since most E_s layers are located below 120 km, their presence there is sustained solely by a vertical shear in the zonal wind or even a westward wind that pushes the plasma downward till it is nearly stopped by collisions. Above 125 km, the process is dominated by a vertical wind shear in the meridional wind, or even by a mere northward wind that

pushes ions down in the upper *E* region, acting as a source of metallics for layer forming at lower altitudes. Finally, as shown by *MacDougall* [1974], no wind component will cause plasma drift below about 98 to 95 km because the vertical Lorenz forces diminish there. In addition, E_s layers start to deplete quickly below this altitude because of sharp increases in metallic ion recombination rates [e.g., see *MacDougall et al.*, 2000].

3. Data and Methods of Analysis

[13] This work was initiated in order to test the validity and generality of the recent findings of *Pancheva et al.* [2003]. The purpose was to identify and study the prevailing periodicities in E_s, which are presumed to be caused by the winds and wind shears associated with atmospheric waves in the lower thermosphere, and then study their properties. To achieve this we considered high-resolution ionosonde E_s critical frequency (*foEs*) time series, from an electromagnetically quiet site during a summer period of fairly continuous sporadic *E* activity, and applied standard analysis techniques used in the study of atmospheric wave dynamics. In order to assess and validate the significance of our findings, the available measurements were supplemented with World Data Center data from a second ionosonde station.

[14] The ionograms used for analysis were obtained with a Canadian advanced digital ionosonde (CADI) which was operated during summer 1996 on the Aegean island of Milos (geographic location 36.7°N, 24.5°). The CADI was programmed to perform a sweep in frequency with 250 steps from 1.5 to 16 MHz in about 54 s and record ionograms every 2 min during the night and 5 min during the day. Inspection of the ionograms showed the presence of a fairly continuous E_s activity from late June to early September, which allowed for a reasonably complete time series of the E_s parameters to be obtained. To materialize this, an interactive program was developed and used to compute the sporadic *E* critical frequency *foEs* in sequence. The layer's critical frequency *foEs* is expressed in MHz and is an estimate of the layer's maximum electron density that is used widely to quantify the layer's strength and variability. Note that although we have also computed the layer's virtual height *h′Es*, this was not used in the present analysis because it can differ significantly at times from the real height due to propagation effects.

[15] To reduce long data ''gaps'' which are due to the absence of layers at times, *foEs* hourly means were computed from 27 June to 4 September, when E_s occurrence was fairly continuous. In this way, the ''no E_s gaps'' represented less than 3% of the total period of 69 days, which, for all practical purposes, is small and expected to have no serious effect on the analysis. In order to have a complete time series, which is required by the wavelet transform algorithm used in our study, the ''no E_s gaps'' were taken as being physically significant, that is, the wind conditions during these times were unfavorable in forming a layer and then filled the gaps with representative values. This was done by replacing the ''no E_s gaps'' during the day by the *E* region critical frequency *foE*, and with the lowest ionogram frequency of 1.5 MHz during the night. In this way we obtained for analysis a complete *foEs* times series of 1656 hourly means for the Milos E_s data during the interval from 27 June to 4 September. In addition, the *foEs* time series of hourly mean values measured by the ionosonde station in Rome (41.9°, 12.5°) for the same exactly time period as the Milos data was also retrieved for analysis from the web page of the Colorado World Data Center.

[16] Since an objective of this work was to determine the prevailing periodicities in *foEs*, the high-resolution spectral analysis method of the ''correloperiodogram'' [e.g., see *Kopecky and Kuklin*, 1971] was selected to compute amplitude spectra. Also, the wavelet transform was employed in order to calculate spectrograms which unravel the dynamic changes in the *foEs* spectral content. Here, the Morlet wavelet was applied, consisting of a sine wave modulated by a Gaussian envelope, which is used widely in the analysis of ionospheric and MLT (mesosphere-lower-thermosphere) wind time series [e.g., see *Pancheva and Mukhtarov*, 2000].

[17] In order to investigate if the observed tidal periodicities are modulated by the dominant PW modes present in *foEs*, a methodology was developed in which the tidal components were extracted by applying a best-fit procedure to the time series. In this respect, the raw data were analyzed by means of using a linear least squares fit method which included the 24-hour, 12-hour, and 8-hour periodic (tidal) components. The data points were weighted in the fitting process according to the number of individual measurements contributing in each hourly mean. The tidal waves were obtained for a time segment of 24 hours, and this segment was shifted through the time series in steps of 1 hour to yield hourly spaced values for the 24-hour, 12-hour, and 8-hour wave amplitudes. The significance of the tidal periodicities was tested by using the Student T-test method to compute confidence levels under the assumption that the residual error in the fit was equivalent of Gaussian-white noise. Finally, the tidal time series were analyzed further by using the wavelet transform method for spectral decomposition in order to identify the dominant modulation periods.

4. Tidal and Planetary Wave Periodicities in E_s

[18] Figure 1 summarizes the Milos *foEs* data in both the time and frequency domain. The upper panel shows the hourly means of the sporadic *E* critical frequency in time sequence from 27 June to 4 September, with the thick line representing a 75-hour running mean. A first inspection of this plot shows the presence of a pronounced diurnal variability which is amplitude-modulated at a much slower rate, from a few to several days. The correloperiodogram amplitude spectrum of the *foEs* time sequence is presented in the lower two panels. The middle panel shows the short period (high frequency) spectrum between 3 and 36 hours, whereas the lower panel has its ordinate axis labeled in days and illustrates the long period spectrum from 1.5 days to 20 days.

[19] The middle panel spectrum is dominated by three narrow spectral peaks fixed exactly at 24, 12, and 8 hours. As seen, the 24-hour peak is by far the strongest whereas the 8-hour component is the weakest. As it will be discussed later, there are good reasons to associate these three periodicities with the diurnal, semidiurnal and terdiurnal atmospheric tides. The bottom panel in Figure 1 shows the *foEs*

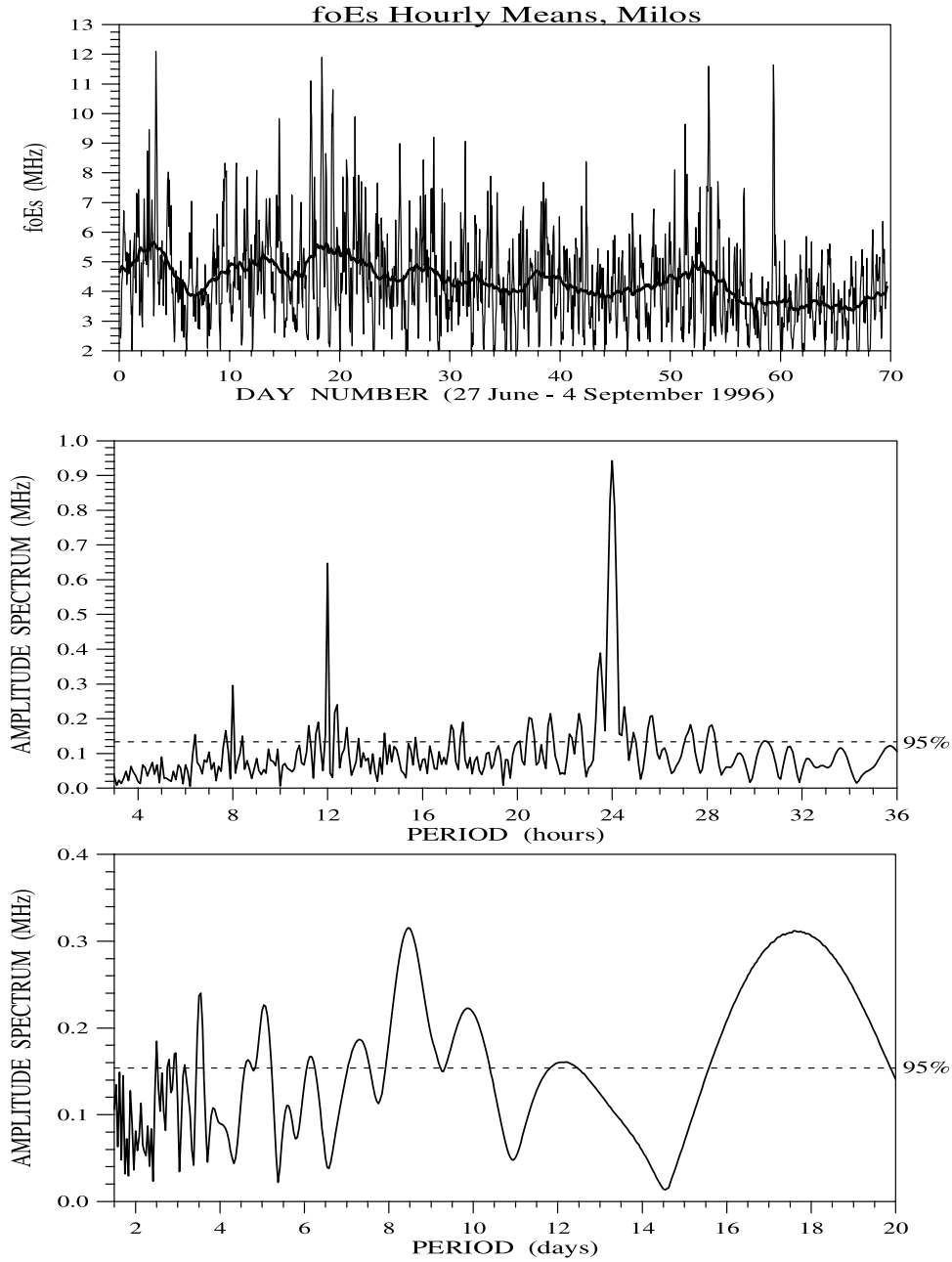

Figure 1. (top) Time series of *foEs* hourly means measured in Milos from 27 June to 4 September 1996; the thick solid line produces the smoothed behavior of *foEs* obtained by a 75-hour running mean. Also shown are (middle) amplitude spectra obtained by the correloperiodogram method for the period ranges from 3 to 36 hours and (bottom) 1.5 to 20 days.

spectrum to intensify in the period range from a few days to about 20 days, with the strongest peaks located between 8.0 to 9.0 days and 16 to 18.0 days. Also, significant peaks that exceed the 95% confidence level exist near 5.0 days and between 2.5 to 3.5 days. In accordance with past studies by *Voiculescu et al.* [2000] and *Haldoupis and Pancheva* [2002], these periodicities are attributable to planetary waves. This is reinforced further by the fact that the geomagnetic variability in the *Ap* index (not shown here), during the summer 1996 interval under consideration, did not exhibit long-term periodicities comparable to the PW-like ones observed in *foEs*. We are aware of course that the PW-like periodicities found in the present data are only approximately close to the usual planetary wave periods predicted by theory, that is, 2, 5, 10, and 16 days. Also, no cross-check has been made here against global PW fields which have undoubtedly been observed by satellites and/or MLT radars during the measurement period under consideration.

[20] The terdiurnal (8-hour) periodicity was identified in ionosonde data clearly for first time. In order to exclude the possibility that the 8-hour peak is the third harmonic of the dominant 24-hour oscillation, we inspected the time series and found the 8-hour variability to be clearly present in *foEs*

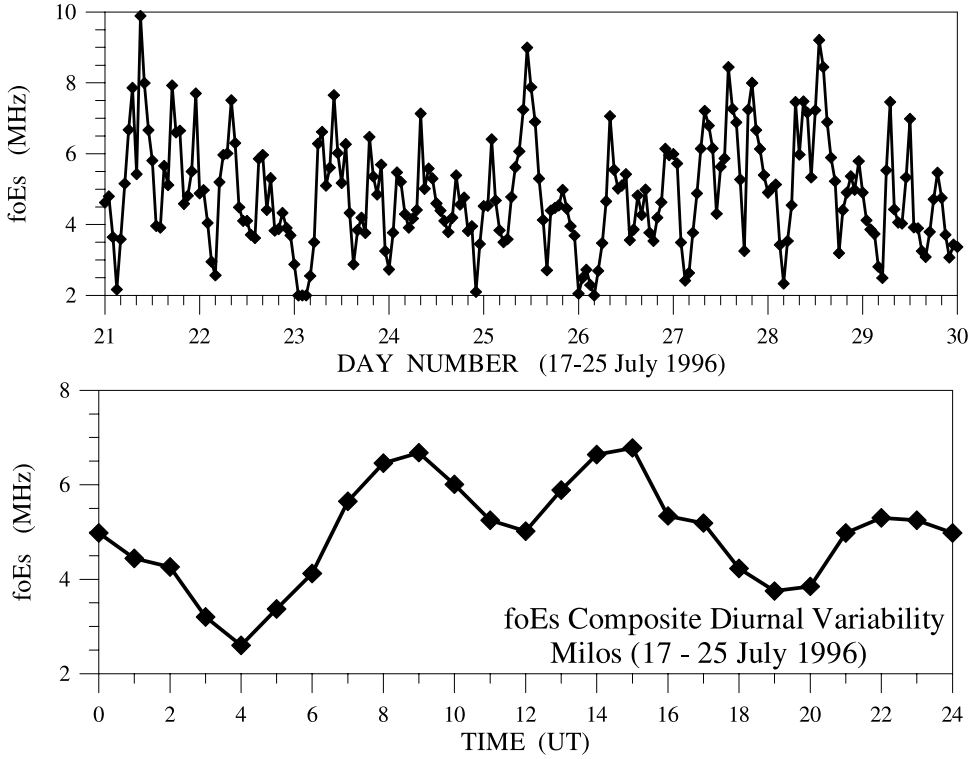

Figure 2. (top) Sporadic layer *foEs* hourly means measured in Milos from 17 to 25 July 1996, where an 8-hour periodicity is prevailing in every day. (bottom) Composite diurnal course obtained by the superposed epoch method for the time interval in the upper panel.

for time intervals of several days. This is illustrated in Figure 2 which shows in the top panel *foEs* hourly means in sequence from day number 21 to 30, that is, from 17 to 25 July 1996. Seen there are three *foEs* peaks present at about 8 hours apart during the course of every day except for day 23. The lower panel displays the mean diurnal variation of *foEs* for all these 9 days shown in the upper pannel, which shows the 8-hour periodicity to be clearly present; thus we conclude that the 8-hour peak in the spectrum is unlikely to be a 24-hour harmonic.

[21] Wavelet period-time-spectrograms of the Milos time series are shown in Figure 3 separately for the 3 to 36 hour band (bottom panel) and the 1.5 to 20 day band (top panel). In accord also with Figure 1, the strongest components are in the short period band, mostly around the 24-hour and 12-hour periods, that is, the diurnal and semidiurnal periodicities in *foEs*. The amplitudes of the tidal-like periodicities however are seen to be strongly modulated in time with a period of several days, and, as expected, they are nearly in phase with the amplitude variations in *foEs* shown in the top panel of Figure 1. The situation here reminds one of the case study of *Pancheva et al.* [2003] and hints of a role played by the PW-like periodicites shown in the upper panel of Figure 3, an option that is dealt with in the next section.

[22] Shown also in the lower spectrogram in Figure 3 are numerous short-lived individual spectral bursts corresponding to oscillations in *foEs* with relatively short periods that compare well with atmospheric gravity wave periods. These components do not peak in the spectrum of Figure 1 (middle panel) because they are uncorrelated; therefore they average out in the correloperiodogram. Finally, the upper panel in Figure 3 shows the presence of a strong 8.5-day oscillation to dominate during the first 25 to 30 days and a weaker 17-day periodicity to be present as well from about day 5 to day 60. In addition, one sees also shorter lasting oscillations with periods less than about 7 days, which can associate with shorter period planetary waves, as it has been concluded elsewhere, for example see *Voiculescu et al.* [1999] and *Igarashi and Kato* [2001].

[23] The same analysis was applied also to the simultaneous Rome *foEs* data and led to similar results. To appreciate the proximity between the Milos and Rome *foEs* periodicities, we provide Figure 4, which is the same as Figure 1 but refers to the Rome ionosonde data. Comparison shows a fair degree of resemblance between the times series (top panels) whereas the amplitude spectra are nearly identical in both the tidal (3–36 hours) and PW (1.5 to 20 days) bands (note that in the lower panel, the dashed line spectrum corresponds to Milos and is plotted here for comparison purposes). A good deal of similarity does also exist between the Milos wavelet spectrograms shown in Figure 3 and the corresponding ones for Rome (not shown here). This suggests that the prominent oscillations imbedded in both the Milos and Rome data are both realistic and significant. On the other hand, their detection in both sites, which are situated about 1300 km apart and differ in latitude by about 5°, implies that a large-scale process is involved, a fact that is in accord with the notion of tidal and planetary wave effects on sporadic *E*.

5. PW Modulation of the Tidal Periodicities

[24] Given that PW amplitudes tend to diminish above about 100 km, *Pancheva et al.* [2003] questioned the direct

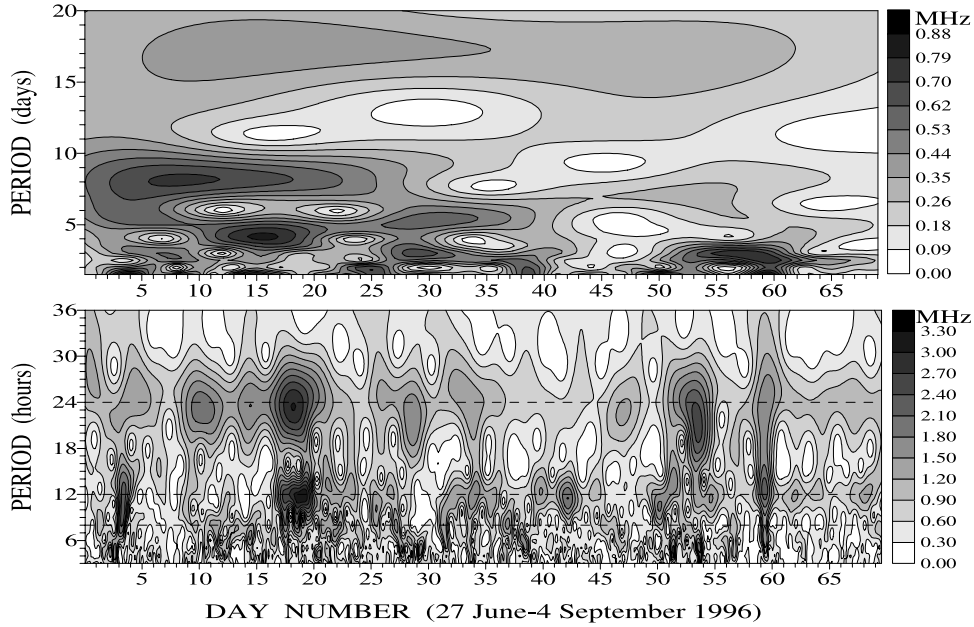

Figure 3. Wavelet spectrograms of sporadic *E* layer critical frequency, *foEs*, measured in Milos from 27 June to 4 September 1996, calculated for the period intervals from (bottom) 3 to 36 hours and (top) 1.5 to 20 days.

PW roll on E_s and provided evidence suggesting an indirect PW role through nonlinear interaction and modulation of atmospheric tides at lower altitudes. The tides, which are known to intensify with altitude and propagate well into the upper thermosphere [e.g., see *Crary and Forbes*, 1986; *Fesen*, 1992; *Mayr et al.*, 1992], carry upwards their PW modulation as well which then is impacted upon E_s through the action of the windshear processes summarized in section 2. In this section we test this option by investigating if the long period amplitude modulation observed in the tidal-like periodicities relates to the PW-like oscillations seen simultaneously in *foEs*.

[25] To examine if the tidal-like periodicities are modulated at the *foEs* PW-like periods, we first extract the tidal components from the data and then compute their wavelet spectrograms. The 24-hour, 12-hour, and 8-hour periodicities were extracted from the *foEs* times series by using the least squares fit method described in section 3. The results of this band-pass filtering process are shown in Figure 5 for all three tidal-like periodicites of the Milos data. As seen, all amplitudes undergo a deep modulation with periods from a few to several days, with the strongest modulation seen in the 24-hour component (upper panel) and the weakest in the terdiurnal one (bottom panel). Also, the amplitude variations are at times in phase for all three components, e.g., see the peak between day 16 and 20 or near day 59.

[26] In order to find if the prevailing modulation periods in tidal amplitudes compare with the PW periods in *foEs*, we compute the wavelet spectrograms of the 24-hour, 12-hour, and 8-hour tidal time series. These are shown in Figure 6. By comparing the spectrograms in Figure 6 and the *foEs* spectrogram shown in the top panel of Figure 3, we conclude the following: (1) Despite differences in detail, there is a general resemblance of all spectrograms. (2) The dominant 8.5-hour PW-like periodicity in *foEs* during the first 25 to 30 days, from about 27 June to 25 July, is also present concurrently in the amplitudes of all three tidal periodicities. (3) A 16-day to 17-day periodicity is present overwhelmingly in the 12-hour amplitude during the first 40 to 50 days, apparently in close relation with the same approximately PW-like period of about 17 days seen in *foEs*. (4) The amplitude of the 24-hour periodicity is strongly modulated at a rate of about 6 to 7 days during the last 30 days of the data, at a time when a similar periodicity is weakly present in *foEs* as well. (5) An amplitude modulation period between 2.5 and 3.5 days is seen in all three tidal components between about day 50 and 65, which coincides with the presence of a periodicity near 3 days seen in *foEs* during the same time. Finally, inspection of the top and bottom panels in Figure 6 suggests that the 8-hour periodicity is not the third harmonic of the 24-hour oscillation.

[27] Given the complexity of the time series and the inherent errors of the analysis methods, the above conclusions support the notion that the tidal periodicities are amplitude modulated at periods which compare well with the simultaneous PW periods present in *foEs*. This is in agreement with the findings of *Pancheva et al.* [2003].

[28] The tidal-PW interaction in the MLT region is known to be a nonlinear process [*Teitelbaum and Vial*, 1991] which resembles amplitude modulation (AM) in communication systems. As a result, one would expect to find about the strong tidal wave peak in the spectrum, two weak secondary peaks at the sum and differences of the interacting primary waves, that is, $\omega_T \pm \omega_{PW}$ for the tidal (ω_T) and planetary (ω_{PW}) waves. Obviously, if we see these secondary peaks to exist in the *foEs* spectrum, then this constitutes evidence in favor of an indirect PW role on E_s through nonlinear interaction and modulation of atmospheric tides.

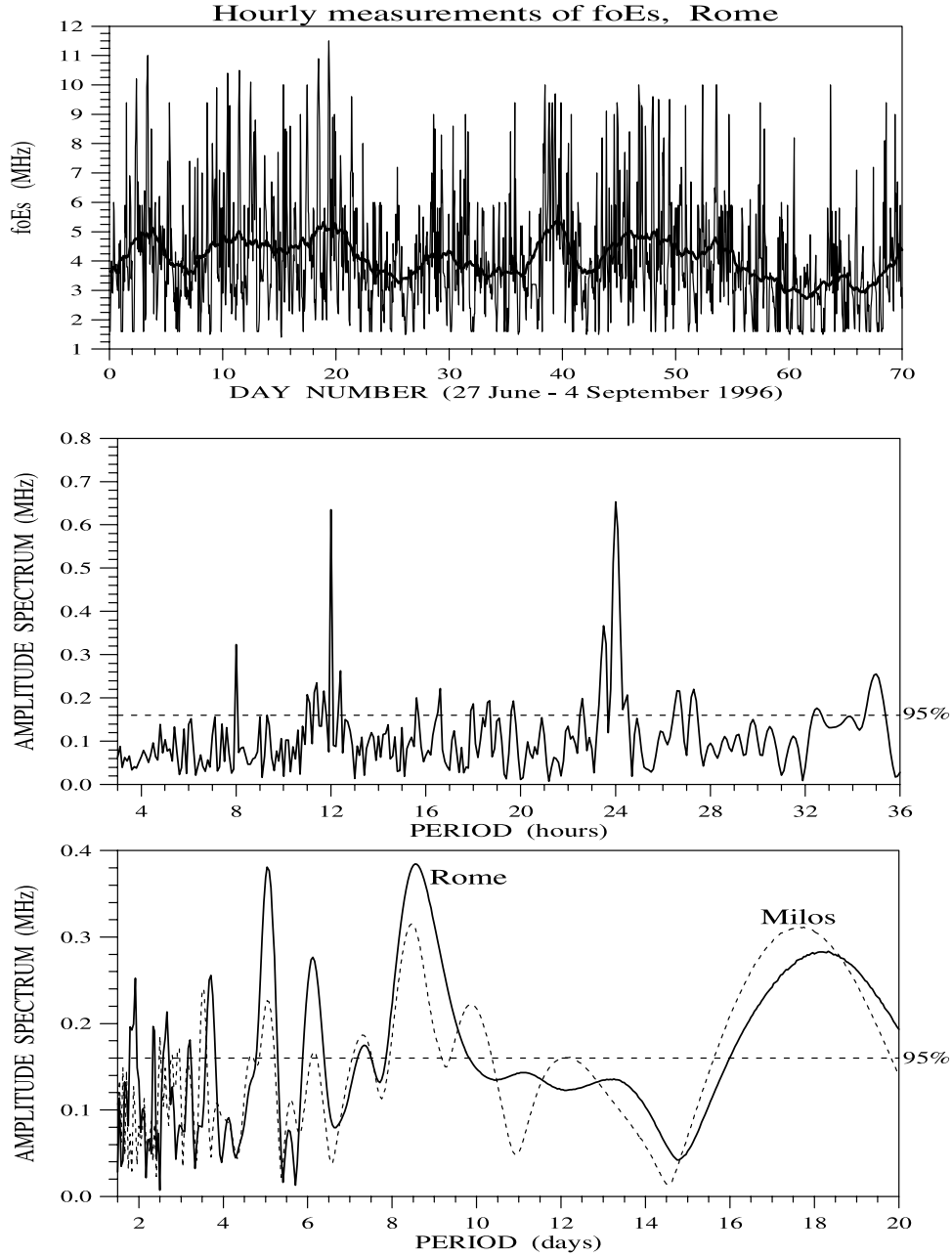

Figure 4. Same as in Figure 1 but for the Rome Ionosonde *foEs* hourly means measured during the same time interval (from 27 June to 4 September 1996) as the Milos observations. For comparison purposes, also plotted in the bottom panel with dashed lines is the corresponding Milos spectrum of Figure 1.

[29] Knowing the dominant PW-like periods in *foEs*, we can search in the spectra for secondary wave peaks about the tidal periods, as it is anticipated from the presumed nonlinear interaction of tides with PW. Based on the wavelet spectrograms of Figures 3 and 6, we observe that the prominent PW-like period bands are centered near 8.5 and 16.5 days during the first 30 days from 27 June to 26 July and near 3 and 7 days during the last 25 days from about 19 August to 4 September. The *foEs* correloperiodogram spectra corresponding to these two time intervals are shown in Figure 7, where the top spectrum is from 27 June to 26 July and the bottom one is from 10 August to 4 September. Also shown in Figure 7 is a number of different arrows designating the position of the secondary peaks computed from the resonance condition $\omega_T \pm \omega_{PW}$, where 1 ω_T are the 24-hour, 12-hour, and 8-hour periods, and $1/\omega_{PW}$ are periods in days of the dominant PW-like periodicities under consideration.

[30] Inspection of the spectra in Figure 7 shows that most of the arrows positioning the anticipated secondary waves under consideration coincide reasonably well with spectral peaks which are statistically significant relative to the 95% confidence level. For example, in the case of the 12-hour component, the secondary waves for the 8.5-day and

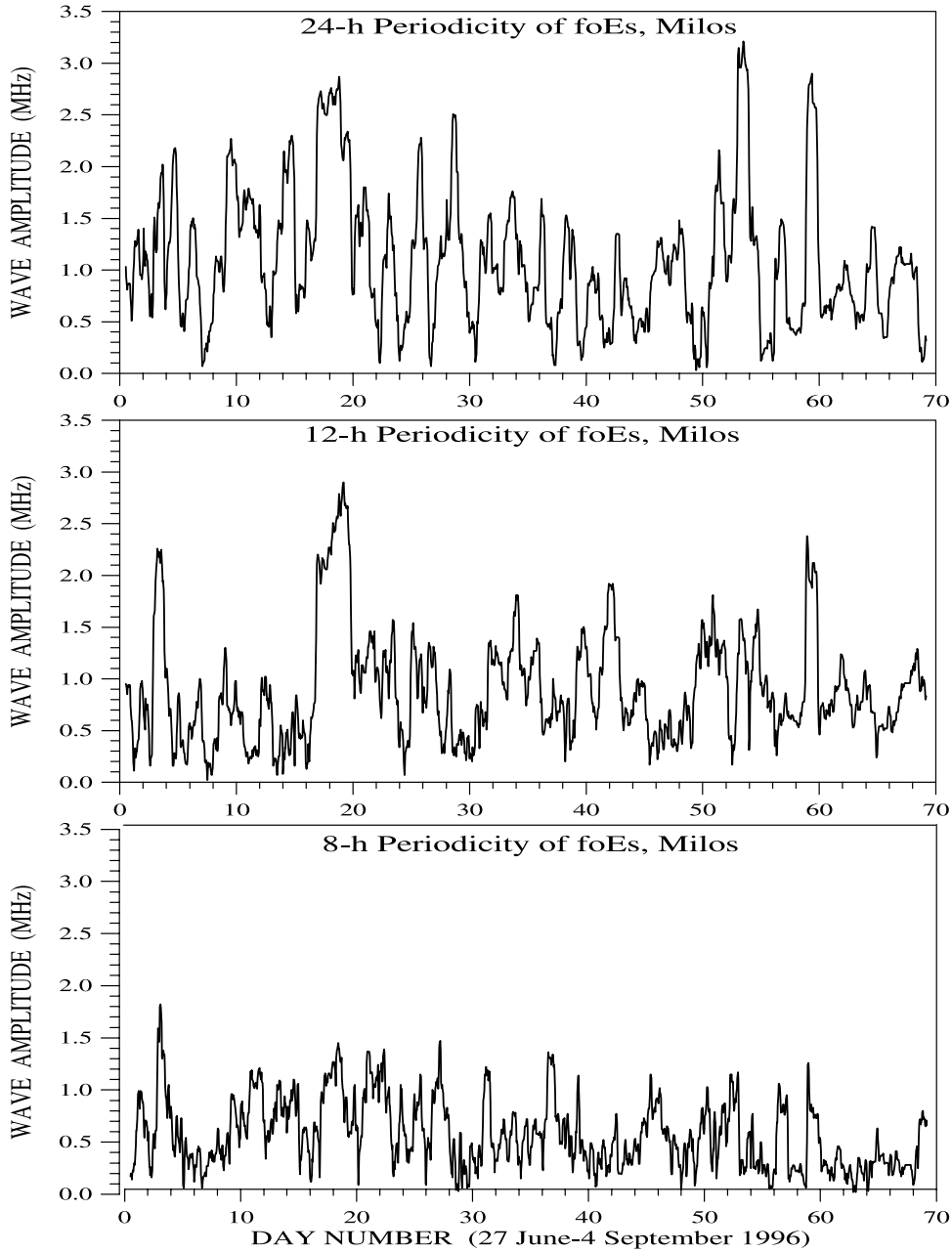

Figure 5. Amplitude variability of the tidal-like periodicities present in the Milos *foEs* time series. Shown are the (top) 24-hour, (middle) 12-hour, and (bottom) 8-hour periodicities extracted from the *foEs* time sequence.

16.5-day PW modulation are near 11.3 and 12.8 hours and near 11.6 and 12.4 hours, respectively. The same is also true for the corresponding Rome spectrum as well (not presented here), showing the semidiurnal *foEs* periodicity to be strongly modulated at about 8.0 and 16.0 days from 27 June to 27 July 1996. Also, for the 24-hour peak during 10 August to 4 September, the secondary waves for the 2.7-day and 7.0-day PW modulation are near 17.5 and 38.0 hours and near 21.0 and 28.0 hours, respectively. As seen, these secondary wave periods are exactly where they should be about the 12-hour and 24-hour tidal peaks in the top and bottom panel of Figure 7, respectively, as designated by the small and large arrows in both panels. The evidence above, although not entirely conclusive, supports the possibility that the modulation of the tidal periodicities results from a nonlinear interaction of atmospheric tides and planetary waves, which again is in line with the results of *Pancheva et al.* [2003].

6. Summary and Discussion

[31] In the present study, continuous time series of critical sporadic *E* frequencies (*foEs*) are analyzed in order to detect and quantify the periodicities impacted upon sporadic *E* by atmospheric wave dynamics. Our results are summarized as follows:

[32] 1. The dominant periodicities in *foEs* are tidal-like and are present regularly and repeatedly. The strongest component is at 24 hours accompanied by a less pro-

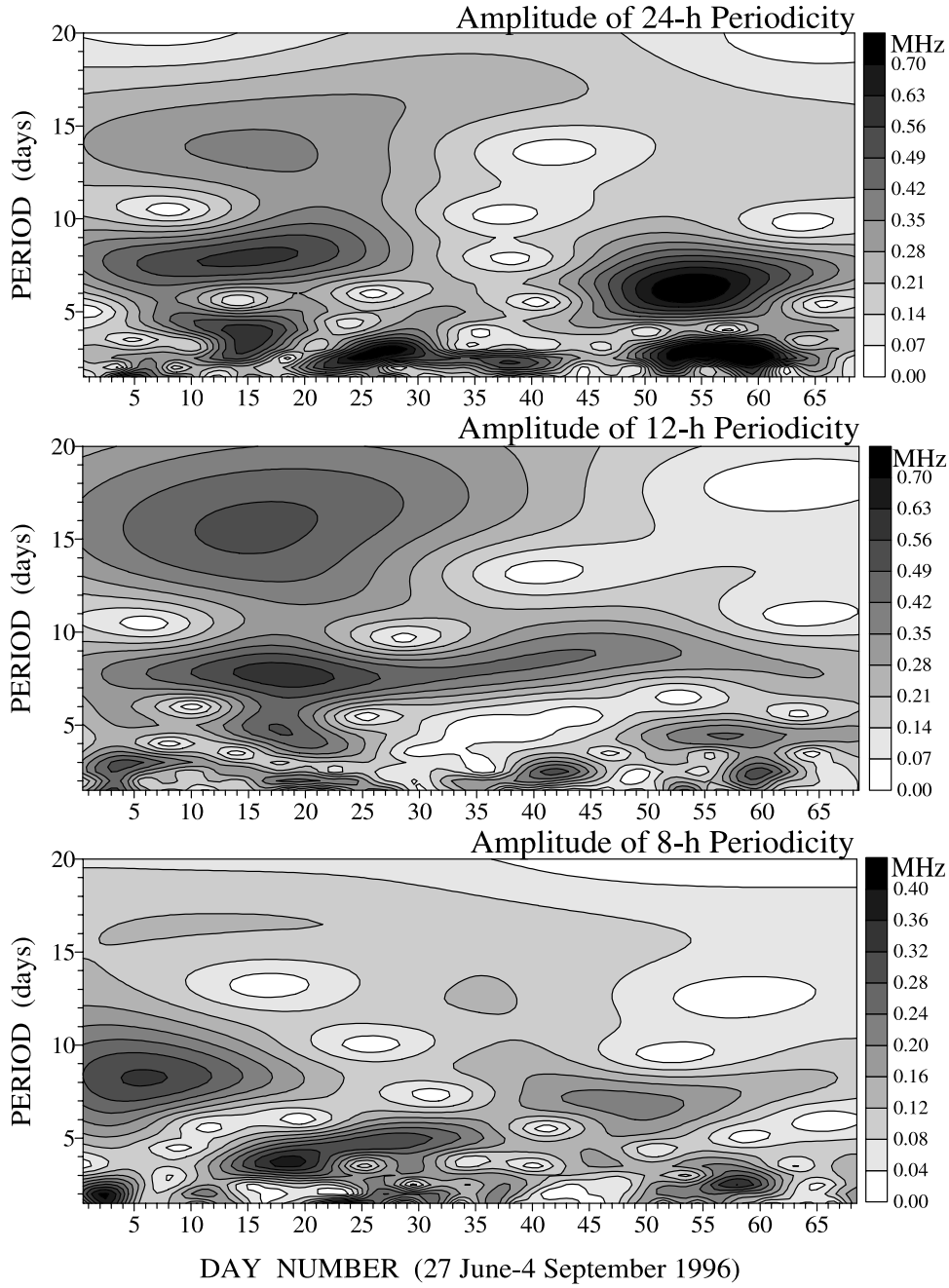

Figure 6. Wavelet transform spectrograms for the amplitudes of (top) 24-hour, (middle) 12-hour, and (bottom) 8-hour periodicities in *foEs* which are shown in Figure 5.

nounced one at 12 hours. These relate to the well-known daily variability of sporadic *E* and are attributable to the diurnal and semidiurnal atmospheric tides in the lower thermosphere. Also detected clearly for first time is a weaker terdiurnal component present as well.

[33] 2. Short lasting bursts of oscillations with periods less than 6 hours, that is, periods comparable to those of gravity waves, are abundant in *foEs* but their occurrence in time is sporadic and uncorrelated.

[34] 3. In accord with recent results, there are significant long-term periodicities present in sporadic *E* as well, having periods in the planetary wave range, that is, near the normal Rossby modes of 2, 5, 10, and 16 days.

[35] 4. The tidal periodicities in *foEs* undergo a long-term modulation in amplitude with periods from a few to many days. These amplitude variations occur mostly simultaneously, and their periods compare well, with the PW-like periodicities in *foEs*.

[36] 5. Some evidence exists indicating that the amplitude modulation of the tidal-like periodicities result from a nonlinear wave interaction process, which could involve planetary waves at lower heights.

[37] The strongest 24-hour and 12-hour periodicities imprinted on sporadic *E* are attributed to the vertical wind structure and propagation of the diurnal and semidiurnal atmospheric tides, which act through the wind shear mech-

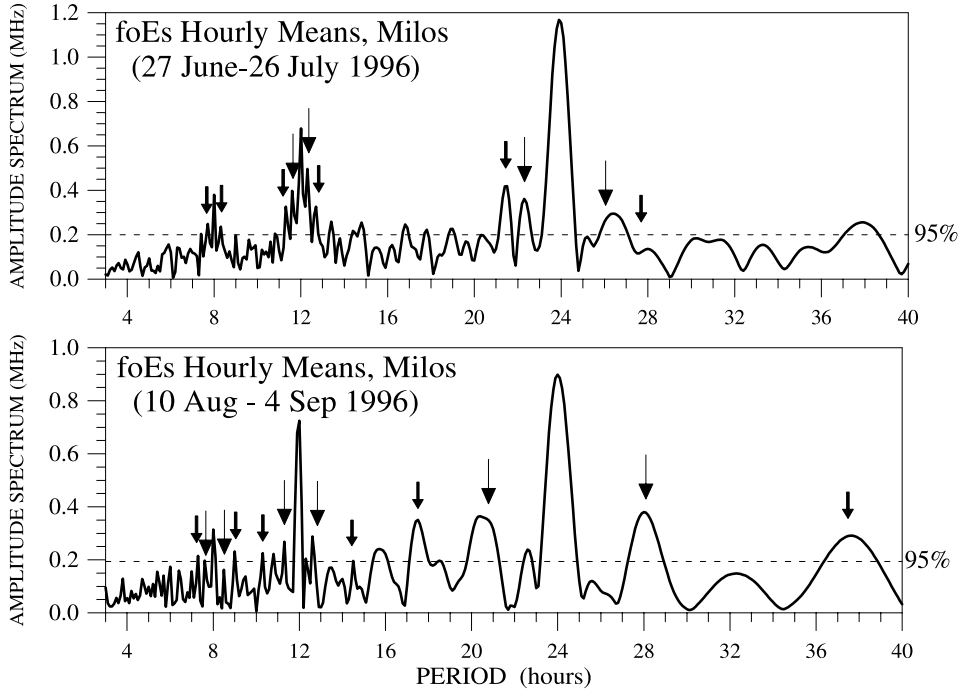

Figure 7. Amplitude spectra of the Milos *foEs* time series for the period range between 3 and 40 hours. The upper spectrum is from 27 June to 26 July; there, the small arrows designate the secondary waves resulting from nonlinear interaction between the *foEs* tidal-like and 8.5-day (PW-like) periodicities, whereas the large (thick) arrows position secondary waves associated with a 16.5-day wave interaction. (bottom) The spectrum for the interval from 10 August to 4 September. There the small arrows indicate the secondary waves resulting from nonlinear interaction between the tidal-like periodicities and a 2.5- to 3-day wave, while the large arrows indicate the interaction with a 6.5- to 7-day wave.

anism outlined in section 2 to produce the layers. Several observations and models show that the tidal winds can control the occurrence and strength of sporadic *E* through their descending vertical wind shears and plasma converging nodes in the altitude range from 100 to 160 km. Apparently, the tidal winds at these altitudes are continuously available for the formation of layers, a fact that has been inferred from the ISR measurements at Arecibo (e.g., see *Mathews* [1998] for a review and a list of references). *Harper* [1977] studied tidal winds in the 100 to 200 km region and found the 12-hour tidal wind system to become dominant above 110 km, whereas it merges into the 24-hour system at altitudes between 100 and 110 km. *Mathews and Bekeny* [1979] presented evidence on the role of the diurnal and semidiurnal tides in forming lower *E* region sporadic *E* and intermediate layers. They noted a repeating semidiurnal pattern for the descending intermediate layers in the upper *E* region and a dominant diurnal behavior for the lower *E* region layers, plus a confluence zone in the lower *E* region where both tidal modes are contributing. Given that the ionosonde E_s reflections are heavily biased to lower altitudes, *foEs* represent mostly heights inside and below the tidal confluence zone, which in turn explains why the observed diurnal periodicity in *foEs* is stronger than the semidiurnal one.

[38] The role of diurnal and semidiurnal tides on E_s formation has been also recognized in several ionosonde studies. *MacDougall* [1974] used a global distribution of ionosondes to infer a well defined role for the zonal semidiurnal and diurnal winds acting near 110 km. The work of *Wilkinson et al.* [1992] and *Szuszczewicz et al.* [1995], who used data from a network of ionosondes as well as simulation models, identified diurnal and semidiurnal tidal modes as the causal mechanisms for layer formation and transport with primary controls driven by meridional and zonal wind-shear forces. In line with inferences made by *Wilkinson et al.* [1992], the regular occurrence and persistence of the tidal periodicities in our data favor a "deterministic" character for E_s which, apparently, is dictated by the permanent global system of thermally driven diurnal and semidiurnal tides.

[39] Our study revealed, in addition to the predominant diurnal and semidiurnal periodicities, a well-defined terdiurnal oscillation in *foEs* which reflects a weaker but regular wave-like process being present. In line with the 24-hour and 12-hour periods, this 8-hour component is identified with a terdiurnal tide in the neutral wind. The literature contains little reference to tide-like oscillations in E_s with periods shorter than 12 hours. *Tong et al.* [1988] have reported an upper *E* region quarterdiurnal (6-hour) oscillation seen by the Arecibo ISR. It was associated with descending intermediate layers and explained in a realistic model atmosphere with a diurnal, semidiurnal, and quarterdiurnal tidal wind system. To our knowledge, *Szuszczewicz et al.* [1995] have the only paper which refers briefly to a possible terdiurnal periodicity seen at times in ionosonde E_s data that was attributed to a descending meridional wind shear associated with a terdiurnal tide in the neutral wind.

Crary and Forbes [1986] refer to terdiurnal tides in the wind field located in the *F* region which were attributed to in situ generation through nonlinear interactive coupling between the neutral wind and ion drag. We feel that the terdiurnal periodicity which seem to appear regularly in *foEs*, is a topic that deserves further investigation.

[40] The observed PW-like periodicities in *foEs* favor the existence of a relation between PW and sporadic *E*, as it was recognized by *Tsunoda et al.* [1998], *Voiculescu et al.* [2000], *Igarashi and Kato* [2001], and *Haldoupis and Pancheva* [2002]. Note that *Igarashi and Kato* [2001] analyzed ionosonde *foEs* measurements and MLT neutral winds obtained with a medium frequency radar at Yamagawa, Japan during August 1996 that overlaps with part of the time interval considered in our study. These authors found PW periodicities of 2, 8, and 16 days in both *foEs* and neutral wind, which agrees at least partly with the PW periodicities observed also in our *foEs* data.

[41] The first effort to understand the physics behind this interaction was made by *Shalimov et al.* [1999], who introduced a mechanism of direct PW-control on the metallic ion density and thus on the E_s forming process. This mechanism, which was formulated and modeled later by *Shalimov and Haldoupis* [2002], required large-scale horizontal convergences of metallic ions in the *E* region, driven by the horizontal Lorentz force inside areas of positive PW vorticity set up by large scale cyclonic neutral wind shears. More recently, *Voiculescu and Ignat* [2003] used a model of linear superposition of tidal and PW wind fields to show that it can lead to PW modulation of metallic ion densities which then can account for the PW-like variations found in E_s layer occurrence. It is important to stress however that these mechanisms are subject to two severe constraints, that is, (1) the PW amplitudes need to be large, which implies PW penetration well into *E* region heights with little attenuation, and (2) the metallic ions need to have long lifetimes of the order of half the PW periods involved.

[42] Recently, *Pancheva et al.* [2003] suggested another physical explanation for the observed relation between sporadic *E* layers and planetary waves. Although this cannot exclude a direct PW role on E_s formation, it showed that sporadic *E* can be affected indirectly by the planetary waves. This was possible through the action of the atmospheric tides which can be strongly modulated by the simultaneously present PW through a nonlinear interaction process at altitudes below 100 km. Evidence on such nonlinear interaction between tides and PW is ample in several MLT wind studies [e.g., see *Pancheva*, 2001, and references therein]. Since the tides are known to intensify in amplitude as they propagate well into the upper *E* region, this mechanism has the advantage to be free of the constraints applying in the case of a direct, or in situ, PW control on E_s.

[43] The present results support the indirect PW mechanism reasonably well. As shown, the long-term, amplitude modulation found in all three (24-hour, 12-hour, and 8-hour) tidal periodicities in *foEs*, varies with time at rates comparable to the periods of the PW periodicities which are present simultaneously in the time series. Also, the analysis provided some additional evidence of an amplitude modulation (AM) process which favors a nonlinear wave interaction. Although we recognize that more testing is necessary, we conclude that the findings of *Pancheva et al.* [2003], which were based on a single PW event, appear to have a general validity.

[44] Finally, we introduced here a new methodology for the investigation of atmospheric wave-induced variability of sporadic *E* layers, in which we have employed analysis techniques used in MLT wind field dynamics. The approach relies on the deterministic character of sporadic *E* which roots in the global system of atmospheric tides and planetary wave climatology. This allows, during the summer months of regular sporadic *E* activity, the detection of fairly continuous times series of the E_s parameters, particularly of the layer's critical frequency *foEs*. We suggest that *foEs* time series can be useful for inferring information on large-scale neutral dynamics at altitudes above 100 km, that is, higher than those covered by conventional (meteor and medium frequency) radar methods. This sounds more promising given the dense network of ionosonde stations and the enormous capacity for continuous global coverage.

[45] **Acknowledgments.** This work was made possible with the support of the European Office of Aerospace Research and Development (EOARD), Air Force Office of Scientific Research, Air Force Research Laboratory under contract FA8655-03-1-3028 to C. Haldoupis, and the Greek Secretariat for Research and Technology and the British Council in Athens through a Greek-British Collaboration Research Grant.

[46] Shadia Rifai Habbal thanks Alain Bourdillon and another referee for their assistance in evaluating this paper.

References

Chimonas, G. (1971), Enhancement of sporadic *E* by horizontal transport within the layer, *J. Geophys. Res.*, *76*, 4578.

Clark, R. R., M. D. Burrage, S. J. Franke, A. H. Manson, C. E. Meek, N. J. Mitchell, and H. G. Muller (2002), Observations of 7-day planetary waves with MLT radars and UARS/HRDI instrument, *J. Atmos. Sol. Terr.*, *64*, 1217.

Crary, D. J., and J. M. Forbes (1986), The dynamic ionosphere over Arecibo, A theoretical investigation, *J. Geophys. Res.*, *91*, 249.

Fesen, C. G. (1992), Tidal coupling between the msosphere and thermosphere, *Adv. Space Res.*, *12*, 27.

Haldoupis, C., and D. Pancheva (2002), Planetary waves and midlatitude sporadic *E* layers: Strong experimental evidence for a close relationship, *J. Geophys. Res.*, *107*(A6), 1078, doi:10.1029/2001JA000212.

Harper, R. M. (1977), Tidal winds in the 100- to 200-km region at Arecibo, *J. Geophys. Res.*, *82*, 3243.

Igarashi, K., and H. Kato (2001), The 2–16 day recurrence cycle of daily sporadic *E* activity and its relation to planetary wave activity observed with MF radar in spring and summer 1996, *Adv. Space Res.*, *27*, 1271.

Kopecky, M., and G. Kuklin (1971), About the 11-year variation of the mean life duration of a group sun spots (in Russian), *Geomagn. Aeronom. Foz. Solntsa*, *2*, 167.

MacDougall, J. W. (1974), 110 km neutral zonal wind patterns, *Planet. Space Sci.*, *22*, 545.

MacDougall, J. W., J. M. C. Plane, and P. T. Jayachandran (2000), Polar cap sporadic-E: Part 2, Modelling, *J. Atmos. Sol. Terr. Phys*, *62*, 1169.

Mathews, J. D. (1998), Sporadic *E*: Current views and recent progress, *J. Atmos. Sol. Terr. Phys.*, *60*, 413.

Mathews, J. D., and F. S. Bekeny (1979), Upper atmospheric tides and the vertical motion of ionospheric sporadic layers at Arecibo, *J. Geophys. Res.*, *84*, 2743.

Mayr, H. G., I. Harris, and W. D. Pesnell (1992), Dynamical interactions between the middle atmosphere and the thermosphere, *Adv. Space Res.*, *12*, 335.

Meyer, C. K., and J. M. Forbes (1997), A 6.5-day westward propagating planetary wave: Origin and characteristics, *J. Geophys. Res.*, *102*, 26,173.

Pancheva, D. (2001), Non-linear interactions of tides and planetary waves in the mesosphere and lower thermosphere: Observations over Europe, *Phys. Chem. Earth C*, *26*, 411.

Pancheva, D., and P. Mukhtarov (2000), Wavelet analysis on transient behavior of tidal amplitude fluctuations observed by meteor radar in the lower thermosphere above Bulgaria, *Ann. Geophys.*, *18*, 316.

Pancheva, D., C. Haldoupis, C. E. Meek, A. H. Manson, and N. J. Mitchell (2002), Evidence of a role for modulated atmospheric tides in the depen-

dence of sporadic *E* on planetary waves, *J. Geophys. Res.*, *108*(A5), 1176, doi:10.1029/2002JA009788.

Shalimov, S., and C. Haldoupis (2002), A model of midlatitude *E* region plasma convergence inside a planetary wave cyclonic vortex, *Ann. Geophys.*, *20*, 1193.

Shalimov, S., C. Haldoupis, M. Voiculescu, and K. Schlegel (1999), Midlatitude *E* region plasma accumulation driven by planetary wave horizontal wind shears, *J. Geophys. Res.*, *104*, 28,207.

Szuszczewicz, E. P., R. G. Roble, P. J. Wilkinson, and R. Hanbaba (1995), Coupling mechanisms in the lower ionospheric-thermospheric system and manifestations in the formation and dynamics of intermediate descending layers, *J. Atmos. Terr. Phys.*, *57*, 1483.

Teitelbaum, H., and F. Vial (1991), On the tidal variability induced by non-linear interaction with planetary waves, *J. Geophys. Res.*, *96*, 14,169.

Tong, Y., J. D. Mathews, and W.-P. Ying (1988), An upper *E* region quarter-diurnal tide at Arecibo?, *J. Geophys. Res.*, *93*, 10,047.

Tsunoda, R., M. Yamamoto, K. Igarashi, K. Hocke, and S. Fukao (1998), Quasiperiodic radar echoes from midlatitude sporadic *E* and role of the 5-day planetary wave, *Geophys. Res. Lett.*, *25*, 951.

Voiculescu, M., and M. Ignat (2003), Vertical motion of ionization induced by the linear interaction of tides and planetary waves, *Ann. Geophys.*, *21*, 1521.

Voiculescu, M., C. Haldoupis, and K. Schlegel (1999), Evidence for planetary wave effects on midlatitude backscatter and sporadic *E* layer occurrence, *Geophys. Res. Lett.*, *26*, 1105.

Voiculescu, M., C. Haldoupis, D. Pancheva, M. Ignat, K. Schlegel, and S. Shalimov (2000), More evidence for a planetary wave link with midlatitude *E* region coherent backscatter and sporadic *E* layers, *Ann. Geophys.*, *18*, 1182.

Whitehead, J. D. (1989), Recent work on mid-latitude and equatorial sporadic-*E*, *J. Atmos. Terr. Phys.*, *51*, 401.

Wilkinson, P. J., E. P. Szuszczewicz, and R. G. Roble (1992), Measurements and modelling of intermediate, descending, and sporadic layers in the lower ionosphere: Results and implications for global-scale ionospheric-thermospheric studies, *Geophys. Res. Lett.*, *19*, 95.

Wu, D. L., P. B. Hays, and W. R. Skinner (1994), Observations of the 5-day wave in the mesosphere and lower thermosphere, *Geophys. Res. Lett.*, *21*, 2733.

C. Haldoupis, Physics Department, University of Crete, Iraklion, Crete, Greece 71003. (chald@physics.uoc.gr)

N. J. Mitchell and D. Pancheva, Department of Electronic and Electrical Engineering, University of Bath, Bath, BA2 7AY UK. (n.j.mithell@bath.ac.uk; eesdvp@bath.ac.uk)